Scanning Microscopy

Volume 2 | Number 1 Article 23

9-2-1987

# Electron Energy Loss Spectroscopic Imaging in Biology

G. T. Simon
*McMaster University*

Y. M. Heng
*McMaster University*

Scanning Microscopy, Vol. 2, No. 1, 1988 (Pages 257-266) 0891-7035/88$3.00+.00
Scanning Microscopy International, Chicago (AMF O'Hare), IL 60666 USA

# ELECTRON ENERGY LOSS SPECTROSCOPIC IMAGING IN BIOLOGY

by G.T. Simon* and Y.M. Heng

Electron Microscopy Facility
Faculty of Health Sciences
McMaster University
1200 Main Street West
Hamilton, Ontario L8N 3Z5, Canada

(Received for publication March 10, 1987, and in revised form September 02, 1987)

## Abstract

One of the goals in biology is to relate the ultrastructure with the movement of elements to understand better physiological and pathophysiological mechanisms. Electron energy loss spectroscopy (EELS) imaging, which was developed in the last decade, appears to be an ideal technique to make such correlation.

EELS takes advantage of the energy distribution of transmitted electrons which interacted with the specimen. All these electrons are collected and can be displayed as an energy loss spectrum for analytical purposes. Images can be produced from selected regions from the energy distribution allowing the mapping of specific elements. The main advantage of EELS imaging in biology is its spatial resolution of 0.5 nm or less and its great sensitivity allowing nearly a single atom detectability. The limitations reside essentially in specimen preparation. In order to obtain optimal results with EELS imaging, only very thin specimens can be used. This restricts the way biological specimens can be prepared. This is a real challenge for the analysis of diffusible elements. Other limitations reside in the difficulty of quantifying the results obtained. This is greatly due to the fact that theoretical considerations still have to be experimentally validated.

The purpose of this review is not to repeat in length the principle of EELS but to emphasize its achievement in biology and to assess the present advantages and limitations. Also, as EELS imaging is still in its development phase, results already obtained are a strong indication that this technique has a great prospect in the analysis of dynamic biological processes.

KEY WORDS:
Electron Energy Loss Spectroscopy, Imaging, Analytical Electron Microscopy, Electron Spectroscopic Imaging, Energy Filtered Image, Microanalysis, Elemental Mapping, Resolution, Inelastic Scattered Electrons, Freeze-Dried Embedding.

*Address for correspondence:
G.T. Simon (Address same as above)
Phone No: (416) 525-9140 Ext.2496

## Introduction

In the last two decades, emphasis was given to elemental analysis in cells and tissues to understand the relationship between chemical activities and the structural organization. To achieve this goal, the requirements are the instrumental capabilities of detecting and displaying the distribution of very small quantities of a given element at high spatial resolution and specimen preparations in order to maintain this element *in situ* without compromising the instrument's ultimate performance.

Despite the progress made in x-ray microanalysis [37,96,97], the visualization of the distribution of a given element related to the ultrastructural organization of tissues and cells is limited by the poor resolution of the system. This is due to the inefficiency of collecting x-ray photons. In addition, the information obtained is due to a secondary or even tertiary signal. Moreover, for low Z elements the yield of x-ray production is reduced due to competing processes such as Auger electron emission [39 (p1-64)]. These disadvantages can be overcome by use of transmitted electrons which can be collected efficiently and analyzed directly. This is the case in electron energy loss spectroscopy (EELS). Electron energy loss spectroscopy takes advantage of the energy distribution of transmitted electrons which have interacted with a specimen. Its applications generally take two forms: display of the spectrum at a selected image point, or acquisition of an image taken from a selected region of the energy distribution.

The principle of EELS has been a review topic in numerous papers [16,18,31(p1-228),42 (p223-244),45,56 (p249-276),63], and its applications in biology has also been discussed extensively in recent years [20,27,46,47,49,71, 95]. Therefore, the purpose of this paper is not another theoretical review but to emphasize the present status of EELS in biology and to assess the related advantages and limitations.

As will be discussed below, several properties of EELS make this electron microscopical analytical technique very useful for the study of biological specimens. These properties are: a) the ability to enhance the

contrast of an image, avoiding heavy metals treatment or staining of the specimen, and still preserve the high spatial resolution; b) the acquisition of images from fairly thick specimens by obviating chromatic aberrations through energy filtration; c) the high efficiency of collecting signals from low to medium Z elements which include many elements that are of biological importance; d) the capability of allowing through elemental mapping the study and construction of molecular structures, and e) the high spatial and mass resolution in microanalysis.

## The EELS Spectrum

The graphical display of the energy loss of electrons scattered by the specimen versus the corresponding electron intensity represents the EELS spectrum (Fig. 1). In a typical EELS spectrum, the first peak (zero loss) is formed by the combination of elastically scattered transmitted electrons which did not lose any appreciable energy (interacting with the nuclear field and thermal vibrations of atoms in the specimen) and electrons which have not been scattered.

The zero loss peak is followed by a series of low energy fluctuations (low loss) due to the electrons which interacted with the valence electrons of atoms in the specimen or electrons in molecular orbitals [36,44,57] and then proceed to form a smooth curve decreasing in intensity concurrently with increasing energy loss. Sharp increases or signals representing the ionization of the inner-shell of an atom are superimposed on this decreasing intensity. These sharp increases take the form of edges rather than peaks. this is due to the fact that electrons ejected from the inner shells can acquire additional kinetic energy in the interaction with the primary electrons. These ionization edges correspond to specific inner-shell binding energies of an element, thus indicating which elements are present within the specimen. The intensities of these edges decrease with increasing inner shell binding energy because of the decreasing cross section. The signal also decreases due to decreasing collection efficiency but this effect can be made small by accepting large scattering angles into the spectrometer or applying higher accelerating voltage to decrease the scattering angle.

In a typical EELS spectrum the pre-edge region generally follows the nature of a power curve ($I = AE^{-r}$ where I is the intensity of electrons which have suffered an energy loss, E is the energy lost, and A and r are constant values which depend on the shape of the curve) [25,65], which can be used to extrapolate the background below an ionization edge. To do this at least two pre-edge intensity readings must be recorded in order to solve for the constants A and r at every point in the curve. After the background has been subtracted from the total signal at the ionization edge, the net elemental signal can be converted to absolute number of atoms and finally concentration [28,31(p229-289), 53,54,56 (p277-299)].

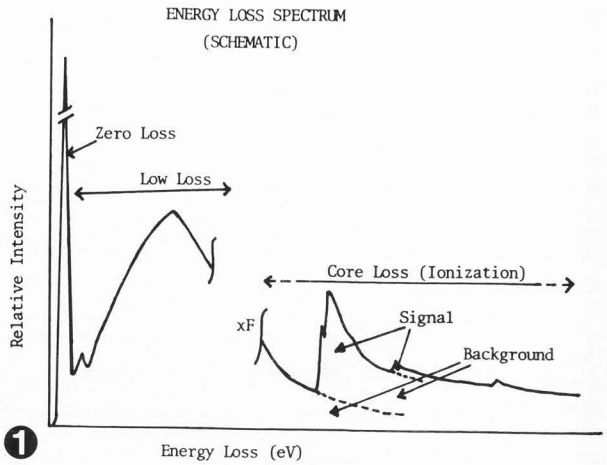


Fig. 1. A schematic energy loss spectrum typical for biological thin sections. The first edge shown here in the core loss region is the characteristic edge for carbon K-shell.

## Spectrometers

The transmitted scattered electrons are dispersed in energy by a spectrometer to form the above-described spectrum. Several EEL spectrometers have been designed and discussed extensively in Egerton's monograph on EELS [31(p27-128)]. Two of them are presently commercially available and will be described here.

The most commonly used is the magnetic prism spectrometer. It consists of a properly designed curved electromagnetic lens capable of dispersing the incoming electrons into a spectrum corresponding to their energies. The magnetic prism spectrometer has the great advantage of being compact and being added as an attachment with no or minor modifications to any CTEM or STEM. Another advantage of the magnetic prism spectrometer consists of the fact that it is not connected to the high voltage system of the microscope. Therefore, higher acceleration voltages can be used. It is, however, essential for any EELS system that the high voltage remains very stable. An energy selected image can be produced with the magnetic prism spectrometer by introducing, after the device, a slit or an aperture. However, EEL spectrometers, like any optical element, suffer from aberrations, particularly "aperture" aberrations which cause a point image to broaden into an aberration figure.

The second type of spectrometer which recently became commercially available is based on the energy-selecting magnetic prism devices which have been introduced by Castaing and Henry [13]. This spectrometer consists of a field magnetic prism and an electrostatic mirror. Electrons deflected by the prism by 90 are reflected through 180 by the mirror passing a second time through the field. These electrons emerge from the prism in the same direction that

they entered. An aperture or slit placed just below the prism allows the passage of only the electrons whose energy lies in a selected range to form a filtered achromatic image. In the last fifteen years this type of filter has been considerably improved by the group of Ottensmeyer in Toronto [40,73]. The prism-mirror spectrometer is installed just above the projector lens and is connected to the high voltage supply. The position of the spectrometer and its dependence on the high voltage prevent it to be readily installed in modern prealigned columns. With this spectrometer, the spectrum or image can be recorded directly on photographic plates or films thus reducing considerably the recording time. With the prism mirror spectrometer, images with a resolution of less than 0.5 nm have been obtained from biological specimens [1,69].

## Elemental Mapping

As mentioned before, the signal which is above the background or the smooth curve of declining intensities represents the characteristic elemental signal. In order to obtain the net elemental signal from the spectrum the background has to be subtracted. Similarly, this can also be done for images in taking at least two EELS images. With both mentioned spectrometers, elemental mapping can be produced by a fixed beam or a scanned beam. Both ways have advantages and disadvantages [31(p124-125)], and are related to electron dose, acquisition time and spatial resolution. In STEM, each pixel is measured in sequence and the values of the background can be extrapolated from values obtained from channels registering the values below the ionization edge and immediately subtracted by computer to give a net elemental pixel [35, 60,61,62]. Another way is to store the pre-edge images and subtract this background from the STEM image containing the total edge signal. The integration of parallel recording of spectra with an efficient computer system provides the simultaneous acquiring and processing of images and also reduces the accumulated dose [10,30,66, 86,90]. The disadvantages are the time of acquisition which is at least a few hundred times longer than in the CTEM due to available electron current limitations and spatial resolution which is related to the probe diameter in STEM.

In the CTEM the simplest method to obtain an elemental mapping is to take an image just below the edge and an image just above the ionization edge and subtract the first image from the second. This can be done photographically [69]. To provide consistency and reproducibility, a region of interest is digitized on the two pictures by a microdensitometer (e.g., 512 x 512 pixels). These images in the form of matrices are then normalized and the subtraction made by computer [3,4]. The disadvantage in using only one picture to determine the background for the subtraction, lies in the assumption that the energy dependence in the spectrum is independent of thickness, density or composition of the preparations. This could lead to inaccurate results and therefore the use of multiple images (more than one pre-edge image) is advocated [18,46,51]. This aspect is particularly important for quantitative considerations [59]. The great advantage of this system is the short acquisition time (frequently not more than 10 sec) and the spatial resolution which, according to the specimens analysed, can be as low as 0.3 nm [69].

## Applications in Biology

EELS imaging can be used for several applications in biology. This subject has been recently reviewed extensively by Jeanguillaume [47]. The possibility to produce an achromatic image (bright field or dark field) improves contrast as well as resolution. The improved contrast is related to the fact that only electrons with energies within the range of the selecting window participate in the image formation. The interrelationship between contrast and resolution then also assures improved spatial resolution [81]. This has been beautifully illustrated by Ottensmeyer [see ref. 74, Fig. 4]. The same area of a thin section was photographed in bright field using all energies, in elastic bright field and in elastic dark field. The two latter images were produced using a prism mirror spectroscopic system. The increase in contrast is dramatic when comparing the bright field image using all the energies with the elastic bright field or the elastic dark field images. In the elastic dark field the resolution and sharpness is even better because only electrons which interacted directly with the preparation are used to form the image without interference by the directly transmitted electrons. This property can be applied to obtain excellent contrast from very thin unstained specimens.

More and more it became evident that conventional fixation using osmium tetroxide ($OsO_4$) denatures proteins and other constituents of cells [32,82]. Several preparation procedures avoiding the use of $OsO_4$ have been proposed and are now almost routinely used [12,23,99]. Fixation at subzero temperatures and embedding in resin at -20 to -70 C is one example. The use of $OsO_4$ has to be banished from preparation to be embedded in low temperature resins because it interferes with polymerization. Thin sections cut from material fixed with glutaraldehyde only and embedded at sub-zero temperature can be readily examined using EELS imaging. The possibility of visualizing ultrastructural details on sections which do not contain any heavy metals fixatives or stains will be of great use, particularly in sections prepared for immunocytochemistry. This is particularly true for labelling labile proteins whose antigenicity can only be preserved by low temperature preparation methods. In addition, avoiding $OsO_4$ fixation and heavy metals staining allow the visualization of substructures normally masked by these metals.

One somewhat unanticipated result is the effect of energy filtration in bright field images of thicker sections. For elastic images, contrast and resolution is improved due to the aforementioned selection of a small energy

window. However, even when this small window is moved into the energy loss spectrum, no contrast reversal is seen due to multiple scattering effects; merely a gradual diminution of contrast is seen, without loss in spatial resolution. These effects, though not yet completely analysed mathematically, have already been used to advantage for specimens with a thickness close to 1 μm [78]. This imaging mode is potentially useful as an alternative to high voltage electron microscopy which has been a popular method for the studies of thick biological specimens [21,33,34,77,79].

The major application of EELS imaging, however, resides in elemental mapping. Research in the elemental composition of biological specimens can be subdivided into two categories: the covalently or tightly bound elements and free electrolytes.

Investigations related to the first group are essentially linked to the study of elements which are an integral part of the structural architecture of cells and tissues. These elements are bound together to form specific structures and are sufficiently stable to be maintained in situ during preparation. In assuming that no denaturation occurred during the preparation, elemental mapping can be used to study the ultrastructural configuration. It is obvious that only certain elements can be mapped for this purpose. For example, the mapping of phosphorus contributed to the understanding of the configuration of DNA, nucleosomes, ribosomes, and even membranes [7,8,36,38,58]. It has been shown that the magnetic energy filter (prism-mirror-prism) gives excellent results in this field of research. The mapping of carbon, which is a universal component of organic material and an integral part of most of the support used to analyze isolated macromolecules, would be futile. Its mapping, however, is of greatest importance to study possible mass loss or contamination due to radiation damages [26,29]. Without underestimating the values of the research made in this first category, which could ultimately lead to the recognition of sequence defects in DNA, RNA and protein synthesis, among others, great emphasis has lately been given to investigation related to the second category.

Investigations related to the second group involve the study of elemental movements and depositions which affect the physiology and pathophysiology of cells and tissues. These elements are coupled to proteins for their transport (e.g., calmodulin as a carrier for calcium) deposited in an insoluble form, or exist in their ionic state.

The studies of ionic concentrations of calcium, potassium, sodium, magnesium and other elements in the different intracellular and extracellular compartments and the study of their movements, are of utmost importance to understand physiological and pathophysiological mechanisms at the ultrastructural level. Among these studies, promising results have been obtained in mapping calcium in striated muscles [69,88,89], and in normal and damaged mitochondria of the proximal renal tubule [92,94]. In the normal mitochondrion, the concentration of calcium is very low (Fig. 2a) and the element appears to be associated with the cristae and the inner mitochondrial membrane. In the mitochondria of epithelial cells of the proximal tubules of kidney subjected to ischemic acute renal failure,

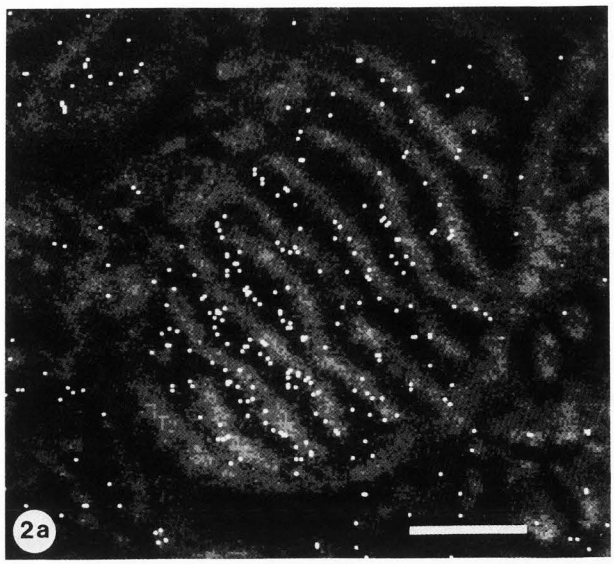


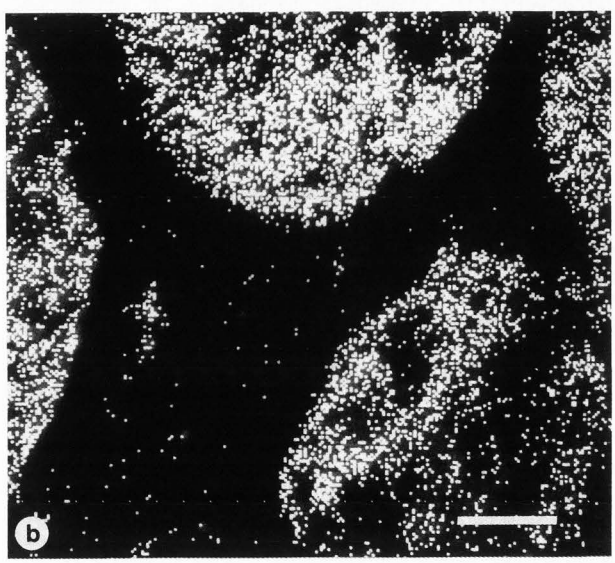


Fig. 2. Calcium L23-edge maps obtained by using one pre-edge image at 320 eV loss as the background reference for the post-edge image at 360 eV loss. In both images (a and b), the net calcium signals are overlaid on energy filtered dark field images. a) A mitochondrion in an epithelial cell of a proximal convoluted tubule in normal kidney; b) portions of mitochondria in a similar region however kidney subjected to ischemic injury. Bars = 100 nm.

the calcium concentration increases with the severity of the lesions and is distributed all over the mitochondria (Fig. 2b). Preliminary studies indicate that some calcium is associated with phosphorus. This might represent the initiation of calcium phosphate crystallization. This was shown by mapping both elements (calcium and phosphorus) and establishing the ratio between them (unpublished results). A list of biological studies using EELS as a tool is given in Table 1.

## Limiting Factors in EELS Imaging for Microanalysis

Present results have shown that under ideal circumstances EELS can detect as low as 3 atoms of Ca [91] and produce images with spatial resolution of 0.3 nm [69]. Theoretical and instrumental limitations in EELS have been discussed in depth by several authors [17,19,50, 52,76]. Therefore, only specimen related factors will be emphasized below.

The limitations in EELS imaging are of several types. Most of them are related to the specimen preparation. A few limitations are directly related to radiation damage and the instrumentation.

It has to be emphasized that the mapping of elements by EELS imaging represents the location and quantity of these elements at the time of analysis but not necessarily in the living state. This is related to specimen preparation, especially for the analysis of diffusible elements which might have been extracted or translocated. In addition, ideally, elemental mapping with EELS should only be performed on very thin specimens which further restricts the way specimens can be prepared and processed. It is accepted that elements in quick-frozen tissue are maintained *in situ* and ideally, frozen hydrated sections should be used for any elemental analysis [37]. Unfortunately, it is presently not possible to obtain thin enough cryosections. Frozen dried sections, which are considerably thinner, show large variation in thickness which makes them not entirely satisfactory yet for EELS imaging. Such specimens necessitate complex processing of the data. This processing remains to be validated. To avoid this complex processing very thin and smoother sections have to be produced. Such sections can only be obtained by cutting specimens from materials quick frozen, dried and embedded in a non-polar resin. This technique has been used and improved by several investigators [15,24,43, 64,92,100]. It is still not entirely proven that diffusible elements are not extracted or translocated during the embedding phase. There is more and more evidence that elements stay in place [43]. The major problem resides in the fact that elements are extracted during cutting when the sections are allowed to float on water. Our recent results indicate that this extraction is true for potassium, sodium and chlorine. It appears, however, that calcium is retained in the sections (unpublished results).

The ideal thickness of biological specimens for microanalysis by EELS or EELS imaging depends on two factors. The first factor is related to

TABLE 1

Summary of EELS applications in biology[a]

| Specimen | Element | S,I[b] | Reference |
|---|---|---|---|
| Amino acids | C,N,O,S | S | 67 |
| Bacteria | P,Ca,N,O | S | 27, |
| | Ca | S | 14 |
| Bone marrow | N,O,Fe | S,I | 46 |
| Cartilage | Ca,P,S, | I | 2,4,5, |
| | Ca,P,Al | I | 3 |
| | Ca,C | I | 59,60,61 |
| Cholesterol | Low loss | S | 36 |
| Diatom | P | I | 73 |
| Exoskeletal Complex (Lobster) | Ca,P,S | I | 6 |
| Ferritin | Fe,C, | I | 87,88,95 |
| | Low loss | S | 36 |
| | Fe | S | 45,68 |
| Golgi | P | I | 11,71 |
| HeLa cells | P,S | S | 27 |
| Hematin | Fe,C,N,O | S | 69,71 |
| Lecithin | Low loss | S | 36 |
| Membrane | Low loss | S | 36 |
| Mitochondria | Ca | I | 92,94 |
| Muscle | Ca | I | 69 |
| | Ca,P | S,I | 85,88,89 |
| | | S | 95 |
| Myelin sheath | P | S,I | 69 |
| Neuron | F,N | I | 59 |
| Nucleic acid bases | C,N,O | S | 44,45,48 |
| Nucleosomes | P | I | 7,8,38,73 |
| Osteoblast | Ca | S,I | 69 |
| Pancreas | C,N | I | 35,60 |
| Plant cells | Si,C,O | I | 71 |
| Platelets | F | S,I | 22 |
| | Ca,P | S | 27 |
| Ribosomes | P | I | 58,73,88 |
| | | S,I | 9 |
| Rough ER | P | I | 11,71,74 |
| Septate junction | P | I | 72 |
| Spectrin | Low loss | S | 36 |
| Synapses | Ca | I | 80 |
| Virus | P | I | 1,69,70 |

[a] More extensive and detail list has been published by C. Jeanguillaume [47]

[b] S = spectrum; I = image

the amount of an element to be analysed. To be detectable, this amount has to give a sufficiently large signal to be recognized above the background noise. The second factor is related to multiple scattering of electrons. In a thick specimen, multiple scattering will produce a reduced characteristic signal on a high uncharacteristic background. It is easy to show from Poisson statistics that the appropriate thickness is one-third of the mean free path of electron scattering, if the multiple scattering error is to be below approximately 15% [75]. Therefore, for biological specimens, section thickness should not exceed 30 nm for 80 kV. In our experience, sections from 5-30 nm in thickness appear to be adequate for EELS mapping of biological material. However, the useful range of specimen thickness increases with increasing beam energy. It has been determined that the mean free path increases with increasing electron energy up to about 500 kV [83,84]. Higher acceleration voltage (above 100 kV) also improves the detection of characteristic inner shell atomic level excitation. Thus improves the signal to noise ratio [41].

Isolated macromolecules constitute ideal preparations for EELS mapping. The thickness rarely exceeds 30 nm, the only limitations being possible beam damage and denaturation of the configuration of the molecules.

In any type of analysis of biological specimens, radiation damage, particularly mass loss, has to be taken into consideration. This mass loss is particularly important for low Z elements which are the most mobile [31(p322-328]. This mass loss may differ considerably from one specimen type to another. Experimental data are necessary to assess this loss for a particular condition and for a given specimen. Reduction of mass loss can be achieved by low temperature analysis, reduction of exposure time, low magnification analysis, efficient signal collection and fast recording time [71]. For long recording times, in particular in the STEM, the stage movement and specimen instability can induce erroneous mapping. A fast computer processing is therefore necessary to reduce the acquisition time. Movements of the specimen and/or stage are of less consequence when a prism-mirror system is used since the acquisition time per image is short. That is, it allows the recording of all image points simultaneously, but images of different energy losses have to be recorded separately, which is the reverse for the STEM system.

Typical exposure time for EELS imaging in CTEM is 2 to 10 sec at a magnification of 40,000X. this corresponds to an exposure of approximately 2 to 10 $Cb/cm^2$. Such a dosage is large compared to the exposure used for very high spatial resolution electron microscopy but it is small by a factor of 10 to 100 when compared to the exposure necessary for x-ray microanalysis.

For any kind of analytical system, the ultimate goal is to be able to quantify the results. This quantification for biological specimens using EELS imaging is a real challenge. All the above-mentioned limitations interfere with it. For example, the thickness of the specimen will affect the signal to background ratio. In a very thin specimen this ratio can be high, while in the thicker specimen with the same concentration of the element, this ratio can be much lower. This phenomenon is due to multiple scattering.

To obtain quantitative results expressed as concentration of an element in a particular compartment of cells or tissues, the thickness and the density of that particular region of the specimen has, therefore, to be known. To date, only approximate values can be estimated for the latter parameter. Finally, the ionization cross-section for a given element in a particular condition must be determined experimentally or theoretically. It has been shown that the experimentally determined cross-section can differ from that obtained theoretically by as much as one order of magnitude [93]. To obtain absolute quantification in EELS imaging, one must be aware of the exact values of each parameter.

In addition to the limitations related to the specimen preparation and instrumentation, the complexity of EELS imaging made its development slow. The introduction of commercially available spectrometers and computer software has not reduced the necessity to have a considerable expertise to process the obtained data. It has to be emphasized that many theories still have to be validated experimentally, particularly for the application of EELS imaging in biology.

## Conclusion

Despite the above mentioned limitations, it has already been demonstrated that EELS imaging is able to produce images with the best spatial resolution obtained on biological specimens. Furthermore, mapping of elements at very high mass resolution was also achieved. The preparation of biological materials for the analysis by EELS imaging still has to be considerably improved. When this is achieved, there is no reason to doubt that EELS imaging will become a method of choice for the study of not only the finest ultrastructural details in cells and tissues, but also to relate these fine structures with the movements of elements in physiological and pathological conditions.

## Acknowledgement

This work was supported by the Medical Research Council of Canada.

## References

1. Adamson-Sharpe KM, Ottensmeyer FP. (1981) Spatial resolution and detection sensitivity in microanalysis by electron energy loss selected imaging. J. Microsc. 122, 309-314.

2. Arsenault AL, Ottensmeyer FP. (1983) Quantitative spatial distributions of calcium, phosphorus, and sulfur in calcifying epiphysis by high resolution electron spectroscopic imaging. Proc. Natl. Acad. Sci. USA 80, 1322-1326.

3. Arsenault AL, Ottensmeyer FP, Hodsman AB. (1983) Spatial distributions of aluminium, phosphorus and calcium in mineralizing epiphyseal

growth plates of aluminium-treated rats by electron spectroscopic imaging. In: Clinical Disorders of Bone and Mineral Metabolism. B. Frame, JT Potts Jr., (Eds.) 220-223.

4. Arsenault AL, Ottensmeyer FP. (1984) Visualization of early intramembranous ossification by electron microscopic and electron spectroscopic imaging. J. Cell Biol. 98, 911-921.

5. Arsenault AL, Ottensmeyer FP. (1984) Stereoscopic representation of complex overlapping element maps in electron spectroscopic images. J. Microsc. 133, 69-72.

6. Arsenault AL, Castell JD, Ottensmeyer FP. (1984) The dynamics of exoskeletal-epidermal structure during molt in juvenile lobster by electron microscopy and electron microscopy and electron spectroscopic imaging. Tissue and Cell 16, 93-106.

7. Bazett-Jones DP, Ottensmeyer FP. (1981) Phosphorus distribution in the nucleosome. Science 211, 169-170.

8. Bazett-Jones DP, Ottensmeyer FP. (1982) DNA organization in nucleosomes. Can. J. Biochem. 60, 364-370.

9. Boublik M, Oostergetel GT, Joy DC, Wall JS, Mainfield JF, Frankland B, Ottensmeyer FP. (1986) In situ localization of ribonucleic acids in biological specimens by electron energy loss spectroscopy. Ann. New York Acad. Sci. 463, 168-170.

10. Bourdilon AJ, Stobbs WM, Page K, Home R, Wilson C, Ambrose B, Turner LJ, Tebby GP. (1985) A dual parallel and serial detection spectrometer for EELS. In: Electron Microscopy and Analysis - 1985, GJ Tatlock (Ed.) Inst. Phys. Conf. Ser. No. 78, 161-164.

11. Brodie DA, Locke M, Ottensmeyer FP. (1982) High resolution microanalysis for phosphorus in Golgi complex beads of insect fat body tissue by electron spectroscopic imaging. Tissue and Cell 14, 1-11.

12. Carlemalm E, Garavito RM, Villiger W. (1982) Resin development for electron microscopy and an analysis of embedding at low temperature. J. Microsc. 126, 123-143.

13. Castaing R, Henry L. (1962) Filtrage magnetique des vitesses en microscopie electronique. C.R. Acad. Sci., Paris, 13255, 76-78.

14. Chang CF, Shuman H, Somlyo AP. (1986) Electron probe analysis, x-ray mapping, and electron energy-loss spectroscopy of calcium, magnesium, and monovalent ions in log-phase and in dividing Escherichia coli B cell. J. Bact. 167, 935-939.

15. Chiovetti R, McGuffee LJ, Little SA, Wheeler-Clark E, Brass-Dale J. (1987) Combined quick freezing, freeze-drying and embedding tissue at low temperature and in low viscosity resins. J. Electron Microsc. Tech. 5, 1-15.

16. Colliex C, Cosslett VE, Leapman RD, Trebbia P. (1976) Contribution of electron energy loss spectroscopy to the development of analytical electron microscopy. Ultramicrosc. 1, 301-315.

17. Colliex C. (1984) Present capabilities and limits of chemical analysis in the electron microscope. In: Electron Microscopy - 1984 (Proc. 8th Eur. Cong. Electron Microsc., Budapest), A Csanady, P Rohlich, D Szabo (Eds.), 1, 349-363.

18. Colliex C. (1984) Electron energy loss spectroscopy in the electron microscope. In: Advances in Opt. and Electron Microsc. R Barer, VE Cosslett, (Eds.) Acad. Press, New York, 9, 65-177.

19. Colliex C. (1985) An illustrated review of various factors governing the high spatial resolution capabilities in EELS microanalysis. Ultramicrosc. 18, 131-150.

20. Cosslett VE. (1980) Progress in electron energy loss analysis for biological specimens. Scanning Electron Microsc. 1980; II: 575-582.

21. Cosslett VE. (1969) High voltage electron microscopy. Quart. Rev. Biophys. 2, 95-123.

22. Costa JL, Joy DC, Maher DM, Kirk KL, Hui SW. (1978) Fluorinated molecule as a tracer: difluoroserotonin in human platelets mapped by electron energy-loss spectroscopy. Science 200, 537-539.

23. Dudek RW, Varndell IM, Polak JM. (1984) Combined quick-freezing and freeze-drying techniques for improved electron immunocytochemistry. In: Immunolabelling for Electron Microscopy. JM Polak, IM Varndell (Eds.) Elsevier Science Publ., New York, 235-248.

24. Edelmann L. (1986) Freeze-dried embedded specimens for biological microanalysis. Scanning Electron Microsc. 1986; IV: 1337-1356.

25. Egerton RF. (1975) Inelastic scattering of 80 keV electrons in amorphous carbon. Phil. Mag. 31, 199-215.

26. Egerton RF, Rossoun CJ. (1976) Direct measurement of contamination and etching rates in an electron beam. J. Phys. D39, 659-663.

27. Egerton RF. (1982) Electron energy loss analysis in biology. In: Electron Microscopy - 1982 Proc. 10th Int. Cong. Electron Microsc., Hamburg. Deutsche Gesellschaft Elektronenmikroskopie, 1, 151-158.

28. Egerton RF. (1982) Principles and Practice of quantitiative electron energy-loss spectroscopy. In: Microbeam Analysis - 1982. KFJ Heinrich (Ed.) San Francisco Press, San Francisco, CA, 43-53.

29. Egerton RF. (1982) Organic mass loss at 100K and 300K. J. Microsc. 126, 95-100.

30. Egerton RF. (1984) Parallel-recording systems for electron energy loss spectroscopy (EELS). J. Electron Microsc. Tech. 1, 37-52.

31. Egerton RF. (1986) Electron Energy-Loss Spectroscopy in the Electron Microscope. Plenum Press, New York, 1-352.

32. van Ewijk W, van Soest PL, Verkerk A, Jongkind JF. (1984) Loss of antibody binding to prefixed cells: fixation parameters for immunocytochemistry. Histochem. J. 16, 179-193.

33. Glauert AM. (1974) The high voltage electron microscope in biology. J. Cell Biol. 63, 717-748.

34. Glauert AM. (1979) Recent advances of high voltage electron microscopy in biology. J. Microsc. 117, 93-101.

35. Gorlen KE, Barden LK, Del Priore JS, Friori CE, Gibson CC, Leapman RD. (1984) Computerized analytical electron microscope for

elemental imaging. Rev. Sci. Instrum. 55, 912-921.

36. Hainfeld J, Isaacson M. (1978) The use of electron energy loss spectroscopy for studying membrane architecture: a preliminary report. Ultramicrosc. 3, 87-95.

37. Hall TA, Gupta BL. (1984) The application of EDXS to the biological sciences. J. Microsc. 136, 193-208.

38. Harauz G, Ottensmeyer FP. (1984) Nucleosome reconstruction via phosphorus mapping. Science 226, 936-940.

39. Hayat MA. (Ed.) (1980) X-Ray Microanalysis in Biology. University Park Press, Baltimore, MD. 1-64.

40. Henkelman RM, Ottensmeyer FP. (1974) An energy filter for biological electron microscopy. J. Microsc. 102, 79-94.

41. Hibino M, Hayashi I. (1986) High voltage electron energy loss spectroscopy evaluated from signal to noise ratio. J. Electron Microsc. 35, 422-425.

42. Hren JJ, Goldstein JI, Joy DC. (Eds.) (1979) Introduction to Analytical Electron Microscopy. Plenum Press, New York, 223-244.

43. Ingram FD, Ingram MJ. (1984) Influences of freeze-drying and plastic embedding on electrolyte distributions. In: Science of Biological Specimen Preparation. JP Revel, T Barnard, GM Haggis (Eds.) SEM Inc, Chicago, AMF O'Hare, IL60666, 167-174.

44. Isaacson M. (1972) Interaction of 24 keV electrons with the nucleic acid bases, adenine, thymine, and uracil (II) inner-shell excitation and inelastic scattering cross-sections. J. Chem. Phys. 56, 1813-1818.

45. Isaacson M, Johnson D. (1975) The microanalysis of light elements using transmitted energy-loss electrons. Ultramicrosc. 1, 33-52.

46. Jeanguillaume C, Tence M, Trebbia P, Colliex C. (1983) Electron energy loss chemical mapping of low Z elements in biological sections. Scanning Electron Microsc. 1983; II: 745-756.

47. Jeanguillaume C. (1987) Electron energy loss spectroscopy and biology. Scanning Microsc. 1:437-450.

48. Johnson DE. (1972) The interaction of 24 keV electrons with guanine and cytosine. Radiat. Res. 49, 63-84.

49. Johnson DE. (1979) Energy loss spectroscopy for biological research. In: Introduction to Analytical Electron Microscopy. J.J. Hren, J.I. Goldstein, D.C. Joy (Eds.) Plenum Press, New York, pp.245-258.

50. Johnson DE. (1981) Limitations to the sensitivity of energy-loss spectrometry. In: Microprobe Analysis of Biological Systems. TE Hutchinson, AP Somlyo, (Eds.) Acad. Press, New York, 351-363.

51. Johnson DW, Spence JCH. (1974) Determination of single scattering probability distribution from plural scattering data. J. Phys. D-7, 771-780.

52. Joy DC, Maher DM. (1980) Electron energy loss spectrometry: detectable limits for elemental analysis. Ultramicrosc. 5, 333-342.

53. Joy DC, Maher DM. (1981) The quantitation of electron energy-loss spectra. J. Microsc. 124, 37-48.

54. Joy DC. (1982) Practical quantitation for energy-loss spectra: a tutorial. Scanning Electron Microsc. 1982; II: 505-515.

55. Joy DC. (1982) Deconvolution for ELS quantitation. Ultramicrosc. 9, 289-294.

56. Joy DC, Romig AD, Goldstein JI. (Eds.) (1986) Principles of Analytical Electron Microscopy. Plenum Press, New York, 249-299.

57. Joy DC. (1986) Quantitative micro-analysis using EELS. In: Principles of Analytical Electron Microscopy. DC Joy, AD Romig, JI Goldstein (Eds.) Plenum Press, New York, 277-299.

58. Korn AP, Spitnik-Elson P, Elson D, Ottensmeyer FP. (1983) Specific visualization of ribosomal RNA in the intact ribosome by electron spectroscopic imaging. Eur. J. Cell Biol. 31, 334-340.

59. Leapman RD, Gorlen KE, Swyt CR. (1984) Background subtraction in STEM energy-loss mapping. In: 42nd Ann. Meeting EMSA. GW Bailey (Ed.), Claitor's Publ. Div. Baton Rouge, LA, 568-569.

60. Leapman RD, Friori CE, Gorlen KE, Gibson CC, Swyt CR. (1984) Combined elemental and STEM imaging under computer control. Ultramicrosc. 12, 281-292.

61. Leapman RD, Gorlen KE, Swyt CR. (1985) Digital processing of electron energy loss spectra and images. Scanning Electron Microsc. 1985; I: 1-13.

62. Leapman RD, Swyt CR. (1985) Quantitative electron energy loss mapping. In: 43rd Ann. Meeting EMSA. GW Bailey (Ed.), San Francisco Press, CA, 404-405.

63. Leapman RD. (1986) Electron energy loss spectroscopy. J. Electron Microsc. Tech. 4, 95-102.

64. Linner JG, Livesey SA, Harrison DS, Steiner AL. (1986) A new technique for removal of amorphous phase tissue water without ice crystal damage: a preparative method for ultrastructural analysis and immunoelectron microscopy. J. Histochem. Cytochem. 34, 1123-1135.

65. Maher DM, Joy DC, Egerton RF, Mochel P. (1979) The functional form of energy-differential cross sections for carbon using transmission electron energy-loss spectroscopy. J. App. Phys. 50, 5105-5109.

66. McMullan D, Williams BG, Sparrow T. (1985) Parallel detection for EELS. In: Electron Microscopy and Analysis - 1985. GJ Tatlock (Ed.) Inst. Phys. Conf. Ser. No. 78, 169-172.

67. Misra M, Egerton RF. (1984) Assessment of electron irradiation damage to biomolecules by electron diffraction and electron energy-loss spectroscopy. Ultramicrosc. 15, 337-344.

68. Nomura S, Todokoro H, Komoda T. (1977) Microanalysis by means of energy loss spectrometry using a field emission STEM. J. Electron Microsc. 26, 277-283.

69. Ottensmeyer FP, Andrew JW (1980) High resolution microanalysis of biological specimens by electron energy loss spectroscopy and by electron spectroscopic imaging. J. Ultrastruct. Res. 72, 336-348.

70. Ottensmeyer FP, Bazett-Jones DP, Adamson-Sharp KM. (1981) Electron energy-loss

microanalysis with high spatial resolution, energy resolution, and sensitivity. In: Microprobe Analysis of Biological Systems. TE Hutchinson, AP Somlyo (Eds.) Acad. Press, New York, 309-324.

71. Ottensmeyer FP. (1982) Scattered electrons in microscopy and microanalysis. Science 215, 461-466.

72. Ottensmeyer FP, Arsenault AL (1983) Electron spectroscopic imaging and Z contrast in tissue sections. Scanning Electron Microsc. 1983; IV: 1867-1875.

73. Ottensmeyer FP. (1984) Electron spectroscopic imaging: parallel energy filtration and microanalysis in the fixed-beam electron microscope. J. Ultrastruct. Res. 88, 121-134.

74. Ottensmeyer FP. (1984) Energy selecting electron microscopy. In: Electron Optical System. SEM Inc., AMF O'Hare, Chicago, IL 60666, 245-251.

75. Ottensmeyer FP. (1986) Scattered electrons in biological structure determination. In: Examining the Submicron World. R Feder, JW McGowan, DM Shinozaki (Eds.) Plenum Press, New York, 137-151.

76. Ottensmeyer FP. (1986) Elemental mapping by electron energy filtration in biology: limits and limitations. In: Proc. XIth Int. Cong. on Electron Microsc., Kyoto, The Japanese Society of Electron Microscopy, Tokyo, 53-56.

77. Parsons DF. (1986) The usefulness of the high voltage electron microscope in biomedical ultrastructure analysis. Ann. New York Acad. Sci. 483, 157-160.

78. Peachey LD, Heath JP, Lamprecht GG, Bauer R. (1987) Energy filtering electron microscopy (EFEM) of thick sections of embedded biological tissue at 80 kV. J. Electron Microsc. Tech. 6, 219-230.

79. Porter K. (1986) High voltage electron microscopy. J. Electron Microsc. Tech. 4, 142-145.

80. Probst W. (1986) Ultrastructural localization of Ca in the CNS of vertebrates. Histochem. 85, 231-239.

81. Rose A. (1973) Vision: Human and Electronic. Plenum Press, New York, 15.

82. Roth J, Bendayan M, Carlemalm E, Villiger W, Garavito M. (1981) Enhancement of structural preparation and immunocytochemical staining in low temperature embedding pancreatic tissue. J. Histochem. Cytochem. 29, 663-671.

83. Sevely J, Perez JPh, Jouffrey B. (1976) Inner shell excitation detection in high energy electron spectroscopy. In: Analytical Electron Microscopy - 1976, Cornell University, Ithaca, N.Y., 167-170.

84. Sevely J. (1985) Voltage dependence in electron energy loss spectroscopy. In: Electron Microscopy and Analysis - 1985. GJ Tatlock (Ed.), Inst. Phys. Conf. Ser. No. 78, 155-160.

85. Shuman H, Somlyo AV, Somlyo AP. (1981) Electron energy-loss analysis in biology: application to muscle and a parallel collection system. In: Microprobe Analysis of Biological Systems. TE Hutchinson, AP Somlyo, (Eds.) Acad. Press, New York, 273-288.

86. Shuman H. (1981) Parallel recording of electron energy loss spectra. Ultramicrosc. 6, 163-168.

87. Shuman H, Somlyo AP. (1982) Energy filtered transmission electron microscopy of ferritin. Proc. Natl. Acad. Sci. USA 79, 106-107.

88. Shuman H, Somlyo AV, Somlyo AP, Frey T, Safer D. (1982) Energy loss imaging in biology. In: 40th Ann. Meeting EMSA. GW Bailey, (Ed.), Claitor's Publ. Div., Baton Rouge, LA. 416-417.

89. Shuman H, Somlyo AV, Safer D, Frey T, Somlyo A.P. (1983) Applications of energy filtered imaging in biology. Scanning Electron Microsc. 1983; II: p.737-743.

90. Shuman H, Kruit P. (1985) Quantitative data processing of parallel recorded electron energy-loss spectra with low signal to background. Rev. Sci. Instrum. 56, 231-239.

91. Shuman H, Somlyo AP. (1987) Electron energy loss analysis of near-trace-element concentrations of Ca. Ultramicrosc. 21, 23-32.

92. Simon GT, Spitzer E. (1985) Freeze-drying-embedding method of specimens for analysis of diffusible elements by electron spectroscopic imaging. In: 43rd Ann. Meeting EMSA. GW Bailey, (Ed.), San Francisco Press, CA, 702-703.

93. Simon GT, Heng YM. (1987) Standards for quantification of elements analysed by energy dispersive spectroscopy (EDS) and electron spectroscopic imaging (ESI). In: Proc. 11th Int. Cong. X-ray Opt. Microanalysis, JD Brown, RH Packwood, (Eds.), 416-419.

94. Simon GT. (1987) Electron spectroscopic imaging. J. Ultrastruct. Path., in press.

95. Somlyo AP, Shuman H. (1982) Electron probe and electron energy loss analysis in biology. Ultramicrosc. 8, 219-234.

96. Somlyo AP. (1984) Compositional mapping in biology: x-rays and electrons. J. Ultrastruct. Res. 88, 135-142.

97. Somlyo AP, Somlyo AV. (1985) Electron probe analysis and cell physiology. In: 43rd Ann. Meeting EMSA. GW Bailey, (Ed.), San Francisco Press, CA, 2-5.

98. Swyt CR, Leapman RD. (1982) Plural scattering in electron energy loss spectroscopy (EELS) microanalysis. Scanning Electron Microsc. 1982; 1:73-82.

99. Tokuyasu KT. (1984) Immuno-cryoultramicrotomy. In: Immunolabelling for Electron Microscopy. JM Polak, IM Varndell, (Ed.), Elsevier Science Publ, New York, 71-82.

100. Wroblewski R, Wroblewski J, Anniko M, Edstrom L. (1985) Freeze-drying and related preparation techniques for biological microprobe analysis. Scanning Electron Microsc. 1985; I: 447-454.

## Discussion with Reviewers

R. Egerton: What do you have in mind by the "complex data processing which remains to be validated'? Is this designed to deal with thick sections or sections whose thickness is non-uniform?

Authors: The expression of 'complex data processing' means the pixel by pixel processing of signals in order to take into consideration the non-uniform section thickness. For thickness

correction, deconvolution of multiple scattering has to be used as proposed by several investigators [51, 55, 61, 91, 98].

R.D. Leapman: As stated by the authors the concentration of calcium in normal mitochondria is very low. In fact, investigators, such as Somlyo et al. [ref. 97], have established for several different cells that the Ca concentration is <1 mmol/kg dry weight (40 ppm). Even in a thin sample the signal/background ratio for the Ca L23 edge would be <0.001. In an embedded section the concentration and S/B would be even lower than this figure. It seems rather surprising therefore that it is feasible to map Ca in the cristae of normal epithelial cell mitochondria as indicated in Figure 2a. Is it possible that mass-thickness effects are responsible for the appearance of calcium in the cristae?
Authors: We agree that with such a low concentration of Ca in normal mitochondria, should the element be evenly distributed in a diluted form, it would be very difficult to detect. However, as shown in figure 2, Ca is not evenly distributed but certain areas are more concentrated than others. The small spatial variation in concentration can only be clearly shown by mapping the element. We are confident that these results are not due to mass-thickness effects because the mapping of P indicates that the location of this element does not necessarily correspond to that of Ca.

R.D. Leapman: Could the authors comment about the practical detection limits for energy spectroscopic imaging of dilute concentrations of elements such as calcium or phosphorus in terms of signal/noise at each pixel in an energy spectroscopic image?
Authors: This is an important question to be considered. We are in the process of determining the detection limits using homogeneous standards.

G.M. Roomans: How were the specimens of which the analysis is shown in Figure 2 prepared?
Authors: The specimens used for mapping Ca in figure 2 were quick-frozen in liquid propane cooled by liquid nitrogen (entrance velocity >6 m/s). The frozen specimens were transferred to liquid nitrogen and then freeze-dried at -130 C for 3 weeks under a vacuum of $10^{-5}$ Torr. The specimens were then gradually brought to 20 C, osmicated with $OsO_4$ vapour and then embedded in Spurr's resin. For elemental mapping, 20 nm thick sections were cut.

G.M. Roomans: What data support your conclusion that "calcium appears to be retained" in the section when it floats on water? Which tissues have been investigated and by what methods?
Authors: We have compared the elemental compositions of dry cut sections with sections cut and floated on water by EDS, which showed the drastic removal of K by water while the Ca signal remained the same. This experiment was done on mitochondria of the $S_3$ segment of kidney in acute renal failure where the concentration of Ca is known to be high and K still detectable by EDS.

G.M. Roomans: Even though data obtained by X-ray microanalysis at organelle resolution seem to show that freeze-drying does not induce ion redistribution, can one exclude ion movements at the higher resolution allowed by EELS (e.g., precipitations of ions on the nearest membrane)?
Authors: In freeze-drying there is no doubt that diffusible elements are attached on the nearest structure, not necessarily membrane. The micro-skeleton and/or proteins are possible sites of such precipitation. This explains why we are able to map Ca in areas where membranes are not present and also indicates that the translocation is minimal.

G.M. Roomans: Would it be possible to check the validity of a Ca map at low Ca concentrations (such as in Fig. 2a) by making, e.g., an Ar map under the same conditions (since Ar is with certainty absent from the specimen)?
Authors: This is possible and it is our intention to use this sort of model as controls. We are currently also testing other methods of signal processing such as using the 2 or more parameters method, to prove the validity of a Ca map. This will also allow accurate quantification of our results.

C. Colliex: Regarding comparison of CTEM and STEM, you obtain the same signal and SNR for one pixel if the same incident dose is used whether it is in a CTEM or a STEM, provided all other factors are supposed to be equal. This is a consequence of the definition of the cross-section:

$$S = N \,.\, J \,.\, \sigma \,.\, \tau .$$

Consider one pixel of dimension d as measured by microdensitometry in the CTEM geometry or defined by the probe size in STEM. Assume d = 1 nm. In this case N is the number of atoms in an area of $d^2$ and thickness t. J is the primary flux of electrons. $\sigma$ is the cross-section. $\tau$ is the recording time. The product $J.\tau$ must be the same in CTEM and STEM cases, i.e., for instance $10^4$ $Cb/cm^2$, as quoted in the text. It can be obtained in 1 ms with a primary flux of $10A/cm^2$ which is typical of a FEG STEM on in 10 s with a conventional gun in a CTEM. These are the only solutions to be compared presently. For 128 x 128 images the total recording time is equivalent in both cases; for increased definition such as 512 x 512, CTEM is more efficient in terms of total recording time.

But clearly the use of CTEM electron spectroscopic imaging is not an advantage in terms of radiation damage, because it is then impossible to record different energy loss images simultaneously. The only solution is the STEM with parallel acquisition of spectrum : the gain in dose radiation is equal to the number of energy loss channels recorded simultaneously.
Authors: We wish to thank Dr. Colliex for his very constructive comments. It is evidently of greatest importance to clarify the immense potential as well as the real limitation of EELS imaging.